Toxicology Reports 2 (2015) 870–879

Contents lists available at ScienceDirect

Toxicology Reports

journal homepage: www.elsevier.com/locate/toxrep

The acidic transformed nano-VO_2 causes macrophage cell death by the induction of lysosomal membrane permeabilization and Ca^{2+} efflux

Shaohai Xu[a], Shengmin Xu[b,*], Shaopeng Chen[b], Huadong Fan[a], Xun Luo[b], Yuxiang Sun[b], Jun Wang[b], Hang Yuan[b], An Xu[b], Lijun Wu[a,b,*]

[a] School of Nuclear Science and Technology, University of Science and Technology of China, Hefei, Anhui, PR China
[b] Key Laboratory of Ion Beam Bioengineering, Chinese Academy of Sciences and Anhui province, Hefei, Anhui, PR China

ARTICLE INFO

Article history:
Received 13 March 2015
Received in revised form 1 June 2015
Accepted 4 June 2015
Available online 10 June 2015

Keywords:
Nanoparticle transformation
Macrophage cell death
Lysosomal membrane permeabilization
Ca^{2+} efflux

ABSTRACT

Because of its outstanding thermochromic characteristics and metal-insulator transition (MIT) property, nano-vanadium dioxide (abbreviated as nano-VO_2 or nVO_2) has been applied widely in electrical/optical devices and design of intelligent window. However, the biological effect of nVO_2 is not well understood, especially when affected by environmental factors or living organisms. For VO_2 is an amphoteric oxide, we simulated pH's influence to nVO_2's physicochemical properties by exposure nVO_2 in water of different pH values. We found that nVO_2 transformed to a new product after exposure in acidic water for two weeks, as revealed by physicochemical characterization such as SEM, TEM, XRD, and DLS. This transformation product formed in acidic water was referred as (acidic) transformed nVO_2). Both pristine/untransformed and transformed nVO_2 displayed no obvious toxicity to common epithelial cells; however, the acidic transformed nVO_2 rapidly induced macrophage cell death. Further investigation demonstrated that transformed nVO_2 caused macrophage apoptosis by the induction of Ca^{2+} efflux and the following mitochondrial membrane permeabilization (MMP) process. And a more detailed time course study indicated that transformed nVO_2 caused lysosomal membrane permeabilization (LMP) at the earlier stage, indicating LMP could be chosen as an earlier and sensitive end point for nanotoxicological study. We conclude that although nVO_2 displays no acute toxicity, its acidic transformation product induces macrophage apoptosis by the induction of LMP and Ca^{2+} efflux. This report suggests that the interplay with environmental factors or living organisms can results in physicochemical transformation of nanomaterials and the ensuing distinctive biological effects.

1. Introduction

The widespread use of engineered nanomaterials has raised concerns about their possible adverse effects to the environment [1,2]. Engineered nanomaterials are deleterious to living organisms [3,4], and have been detected in the environment within some place at a relative high concentration [5–7]. Studies have indicated that the property and property-related toxicity of nanomaterials changed significantly after released into environment and interplayed with environmental factors and organisms. For instance, fullerene underwent surface oxidation and transformed to soluble product upon exposure to ultraviolet or sunlight [8,9]; in aquatic environment, nano-Ag was easily oxdiatied and formed a sulfidation layer on its surface [10,11]; and nano-ZnO underwent ageing and changed its toxicity [10]. Thus, it is vitally important to study the physicochemical change of nanomaterials under environmental factors and the ensuing distinctive biological effects.

Nano-vanadium dioxide (nano-VO_2) possesses metal-insulator transition (MIT) property, which makes it an attractive material for applications in electrical/optical devices, such as display devices, light storage devices, optical switch, bolometer, and intelligent window [11]. Although the biological effect of nano-scaled VO_2 is poorly understood, research on vanadate ions and compounds containing vanadium is long-standing [12,13]. The bulk of the vanadium in mammalian is in the vanadyl (IV) form (VO^{2+} ions), which binds tightly to proteins; vanadate ions can mimic the effect of insulin and promote glucose oxidation in adipocytes [14]. Chemical compounds containing vanadium (V) potently inhibits (Na^+–K^+) ATPase in red blood cells [15]. And the peroxovanadium compounds serve as phosphotyrosine phosphatase inhibitors and mediate apoptosis in B lymphocytes [16].

* Corresponding authors at: Key Laboratory of Ion Beam Bioengineering Hefei Institutes of Physical Science, Chinese Academy of Sciences Hefei, Anhui 230031, PR China. Fax: +86 551 65595670.

http://dx.doi.org/10.1016/j.toxrep.2015.06.005

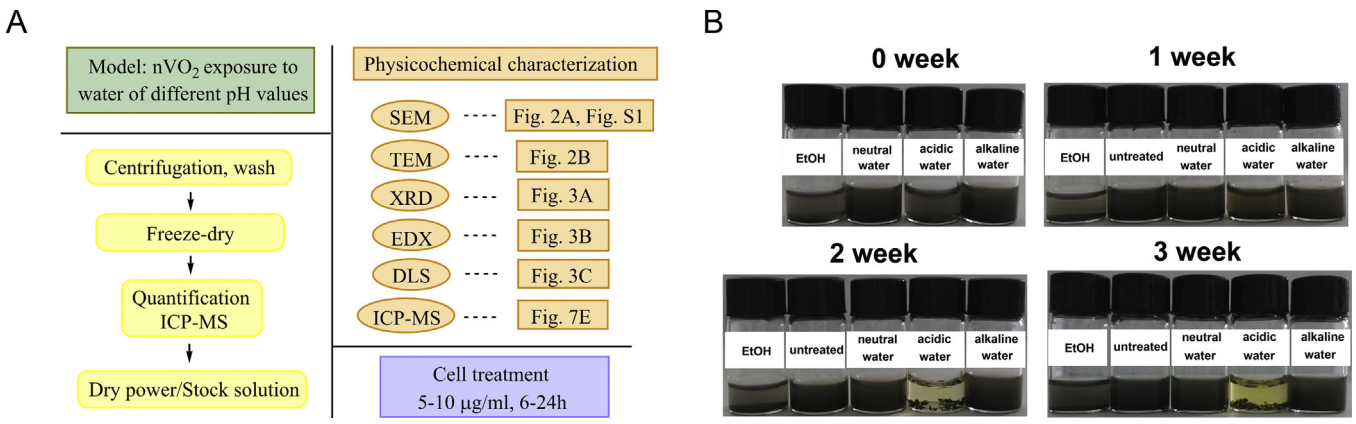

Fig. 1. nVO_2 transformed in acid water. (A) The experimental procedure of simulating the transformation of nVO_2 under the environmental and organisms' condition. (B) nVO_2 was dissolved in water with different pH values (pH 7, 5, 9) and was kept for 3 weeks (at a final concentration of 10 or 100 μg/ml). Pictures were taken every week. For visible to the unaided eye, experiment on 100 μg/ml was displayed here. Representative of at least 3 independent experiments ($n \geq 3$).

For nano-scaled VO_2, generally asked question is that whether it induces diverse biological effects on different biological systems. Research has displayed that nVO_2 induces autophagy in an epithelial cell line [17]. And nano-scaled vanadium oxide (V_2O_3) causes distinct biological effect to different cells, such as ECV304, A549, and RAW264.7 [18]. Here we asked whether nVO_2's physicochemical properties affects its biological effects, because nVO_2 is an amphoteric oxide which may easily form coordination compound on its surface under relevant environmental conditions such as pH. It has been reported that pH significantly affected the stability and dissolution of ZnO nanoparticles in aqueous solutions [19]. And the toxicity of ZnO nanoparticles to *Eisenia fetida* was highly influenced by pH [20].

To fully understand nVO_2's potential risk to the organisms, we simulated pH's influence to nVO_2 by exposure nVO_2 in water of different pH values. Our results demonstrated that nVO_2 in acidic water formed new transformation product after two weeks. Importantly, acidic transformed nVO_2 rapidly induced apoptosis in macrophages through the induction of lysosomal membrane permeabilization (LMP) and Ca^{2+} efflux. We suggest that the interplay with environmental factors or living organisms can results in physicochemical transformation of nanomaterials and the ensuing distinctive biological effects.

2. Materials and methods

2.1. Preparation of nVO_2

Synthesis of nVO_2 was performed with a simple strategy, which is low-cost and large scale, by combining hydrothermal synthesis with a subsequent mild thermal treatment [11]. Endotoxin levels of nanomaterials (pristine or transformed nVO_2) were about 0.1 EU/mL (<0.25 EU/ml), measured as previously described [21].

2.2. Cells and reagents

The mouse monocyte/macrophage cell line RAW264.7 and human embryonic kidney cell line HEK293T were obtained from the American Type Culture Collection (ATCC, Rockville, MD, USA). For obtain of bone marrow-derived macrophage (BMDM), bone marrow cells were isolated from femurs and tibiae of 6-8 week-old C57BL/6 mice, and cultured in 1640 complete medium containing conditional media from L929 cell culture as described previously [22]. After 24 h, non-adherent cells were transferred to a new plate and fresh L929 conditional medium was added every other day. BMDM were harvested at day 7, when they expressed common macrophage surface markers such as CD11b and F4/80. Cells were cultured and maintained in RPMI-1640 containing 10% FBS, 100 U/ml penicillin, and 100 μg/ml streptomycin (Invitrogen, San Diego, CA, USA). Mice were housed under specific pathogen-free conditions at School of Life Sciences, University of Science and Technology of China (USTC). Animal care and experimental procedures were in accordance with the experimental animal guidelines at USTC.

RAW264.7 cell line was employed to study the toxicity and toxicity mechanism. HEK293T cell line and the induced primary macrophage BMDMs were employed to study the cytotoxicity.

3. Experimental procedure (nVO_2-pH treatment, characterization, and cell treatment)

As shown in the schematic diagram in Fig. 1A, the experimental procedure contains four parts:

(1) nVO_2 exposure to water of different pH values. We dissolved nVO_2 in acidic, neutral, and alkaline water; the pH value of Milli-Q water was adjusted as previously described [23,24]. The pH values chosen here (pH 5–9) were in relevant to both the environmental and organisms' condition; other extreme pH-treated group was displayed in Fig. S1. Both nVO_2's final concentration of 10 and 100 μg/ml displayed the same results. The exposure time was from 1 to 3 weeks, and last for half a year.

(2) Obtain of pH-treated nVO_2. nVO_2 was take out of water by centrifuging tubes at 100,000 rpm for 5 min, washing with water for three times, and freeze-drying with a lyophilizer [11]. The dry power was used for physicochemical characterization, or quantitated by ICP-MS and dissolved to form a stock solution (100 μg/ml) for cell treatment.

(3) Physicochemical characterization. The morphology, microstructure, phase structure, and composition of the nVO_2 were examined, respectively, using Field-Emission Scanning Electron Microscopy (FESEM; Sirion 200), Transmission Electron Microscope (TEM; JEOL-2010), X-ray Diffraction with the Cu $K\alpha_1$ line (XRD; Philips X'Pert), and Energy Dispersive X-ray (EDX, AN1085; Oxford Instruments). Dynamic Light Scattering (DLS) Size (Hydrodynamic diameters) and Zeta Potential under typical exposure conditions were measured by a Zetasizer Nano-ZS instrument (ZEN3600, Malvern Instruments). Inductively Coupled Plasma Mass Spectrometry (ICP-MS, X Series 2, Thermo fisher Scientific) was employed to determine the vanadium content in cells [11,25,26].

(4) Cell treatment/toxicity study. nVO_2 was diluted to 5 or 10 μg/ml in fresh medium (RPMI-1640 containing 10% FBS), and

then added to cells [27]. It takes only 24 h to determine the toxicity and toxicity mechanisms in our study. For separation with nVO_2, cells were sorted by flow cytometry (BD FACSAria III).

4. Cell viability assay

Trypan blue exclusion assay and MTT assay were performed as described [27]. Trypan blue solution (0.4%) was from Sigma–Aldrich; cells were calculated by Countstar IC1000 (Inno-Alliance Biotech). For MTT assay, MTT was added to each well after treated with nanomaterials at a final concentration of 0.5 mg/ml. Absorbance at 590 nm (A590) was determined using a microplate reader.

4.1. Cell death assay

After treated with nanomaterials, cells (RAW264.7) were subjected to fluorescein isothiocyanate (FITC)-conjugated annexin V and propidium iodide (PI) staining according to Annexin V: FITC Apoptosis Detection Kit (556,547, BD Pharmingen™, San Diego, CA, USA), then apoptotic and dead cells were analyzed by flow cytometry.

Sub-G1 cell (apoptosis) populations were assayed using PI staining as previously described [28]. Cells were washed with PBS and fixed with 70% ethanol at 4 °C overnight. Later, cells were washed and resuspended with PBS containing 0.2% Triton X-100 and 100 μg/ml RNase A, and then stained with 50 μg/ml PI at 4 °C for 30 min.

4.2. Cytosolic calcium measurement

Rising cytosolic calcium concentration, which indicated changes in cell signals or fate, was measured by the calcium-sensitive dye FLUO3-AM [29]. Briefly, RAW264.7 cells were incubated in RPMI-1640 containing 10% FBS and pretreated with 1 μM FLUO3-AM (Invitrogen-Molecular Probes, San Diego, CA, USA) at 37 °C for 2 h. Cells were harvested at various time points (0, 6, 9, 12, 15, 18 h), and the cytosolic calcium levels were determined by flow cytometry (FLUO3-AM: excitation wavelength, 506 nm; emission wavelength, 526 nm, monitored at FL-1 channel) [29].

4.3. Assessment of $\Delta\psi_m$ drop

Loss of mitochondrial transmembrane potential ($\Delta\psi_m$), which indicates a later ongoing mitochondrial membrane permeabilization (MMP) and cell death, was measured by employing Mitochondrial Membrane Potential Detection Kit (551,302, BD Pharmingen™, San Diego, CA, USA) [30]. Briefly, RAW264.7 cells were incubated with 5 μg/ml of JC-1 for 10 min at 37 °C; cells were assayed by flow cytometry. Cell population with a decrease in red fluorescence was gated out and regarded as the subpopulation with impaired mitochondria and $\Delta\psi_m$ drop [30].

4.4. Acridine orange relocation assay

Acridine orange relocation assay demonstrating lysosomal damage was performed as described [31]. Briefly, RAW264.7 cells were seeded in 6-well plates with 5×10^5 cells/well and cultured for 12 h. After that, 5 μg/ml of AO (Invitrogen-Molecular Probes, San Diego, CA, USA) was added to plates and incubated for 15 min. Then, cells were washed twice with PBS and treated with nanomaterials. After treatment, cells were collected at 6 or 12 h, washed three times with PBS, fixed with 4% paraformaldehyde, and then were subjected to assessment of red (FL-3 channel) and green (FL-1 channel) AO fluorescence using flow cytometry.

4.5. Lysotracker staining

Lysotracker dye labels acidic spherical granules and will continue to stain lysosomal membranes that undergo LMP within cells [31]. RAW 264.7 cells (1×10^5/ml) were incubated with 1640 complete medium containing 50 nM Lysotracker Green (Invitrogen-Molecular Probes, San Diego, CA, USA) at 37 °C for 60 min, washed twice, and then treated with nanomaterials [31]. After treatment, cells were assayed by flow cytometry.

4.6. Flow cytometry analysis

Cells were resuspended (1×10^6 cells/ml) in staining buffer (PBS with 10% FBS), stained with fluorescent dye and washed with PBS. Analyses were performed on the FACSCalibur (BD, San Diego, CA, USA) and analyzed with FlowJo software (Tree Star, Ashland, OR, USA).

4.7. Statistics

All data were expressed as mean ± standard error of the mean (SEM). P values were generated using two-tailed student's t-test ($^*P \leq 0.05$, $^{**}P \leq 0.01$, $^{***}P \leq 0.001$).

5. Results

5.1. The physicochemical characterization of nVO_2 transformation in acidic water

Metal oxide nanoparticles have been used in all aspects of human life and social production, leading to an increased interest of their behavior affected by environmental factors and organisms' process [32]. pH, an important factor, could influence the stability, aggregation, and dissolution of nano metal oxides, both under environmental and organisms' condition [19]. In order to reveal the influence of pH to nVO_2's physicochemical properties and biological effects, we first simulated pH's impact on nVO_2 by exposure nVO_2 in water of different pH values. The experimental model was displayed in schematic diagram (Fig. 1A). nVO_2 was kept in water of different pH values for different time (Fig. 1B). We found that nVO_2 in acidic water (10–100 μg/ml) formed flocculus unapparently at the beginning of first 10 days, and there was obvious aggregated mass of flocculent material suspended in the acidic water after two weeks (Fig. 1B) (For visible to the unaided eye, experiment on 100 μg/ml was displayed here).

We characterized the acidic transformed nVO_2 using different methods. SEM study displayed that the morphology was affected after exposure to acidic or neutral water for two weeks (Fig. 2A), and eight months' exposure displayed that nVO_2 transformed to colloid-like V_2O_5 (Fig. S1). Using TEM to further study the mass of flocculent material and determined the microstructure and surface change, we revealed that nVO_2 aggregated together to form a new transformation product after exposure in acidic water for two weeks (Fig. 2B). For short-term exposure (less than one week), we did not observe this transformational change. And DLS assay demonstrated that the acidic transformed nVO_2 displayed distinct particle size and Zeta potential (Fig. 3C and D).

Next, using XRD and EDX, we revealed that the phase structure, elementary composition, and vanadium-oxygen ratio of acidic transformed nVO_2 (exposure for two weeks) had no obviously change, indicating that the acidic transformed nVO_2 was not oxidized to V_2O_5 (Fig. 3A and B). Therefore, nVO_2 undergoes physicochemical transformation after two weeks' exposure in acidic water.

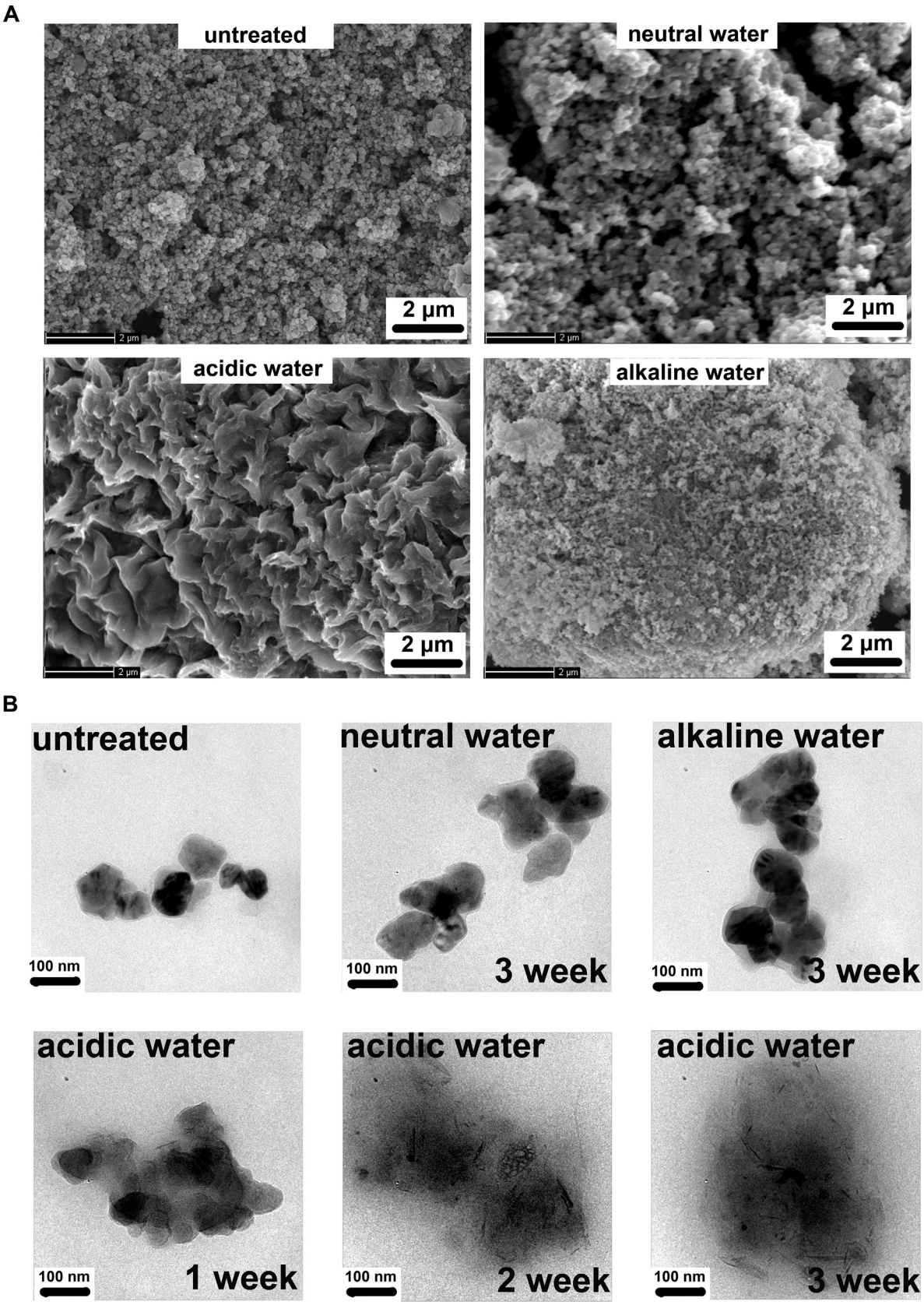

Fig. 2. Characterization of nVO_2's transformation products by SEM and TEM. The surface morphology and microstructural characterization of nVO_2's transformation products (exposure for two weeks) were performed on SEM and TEM, respectively.

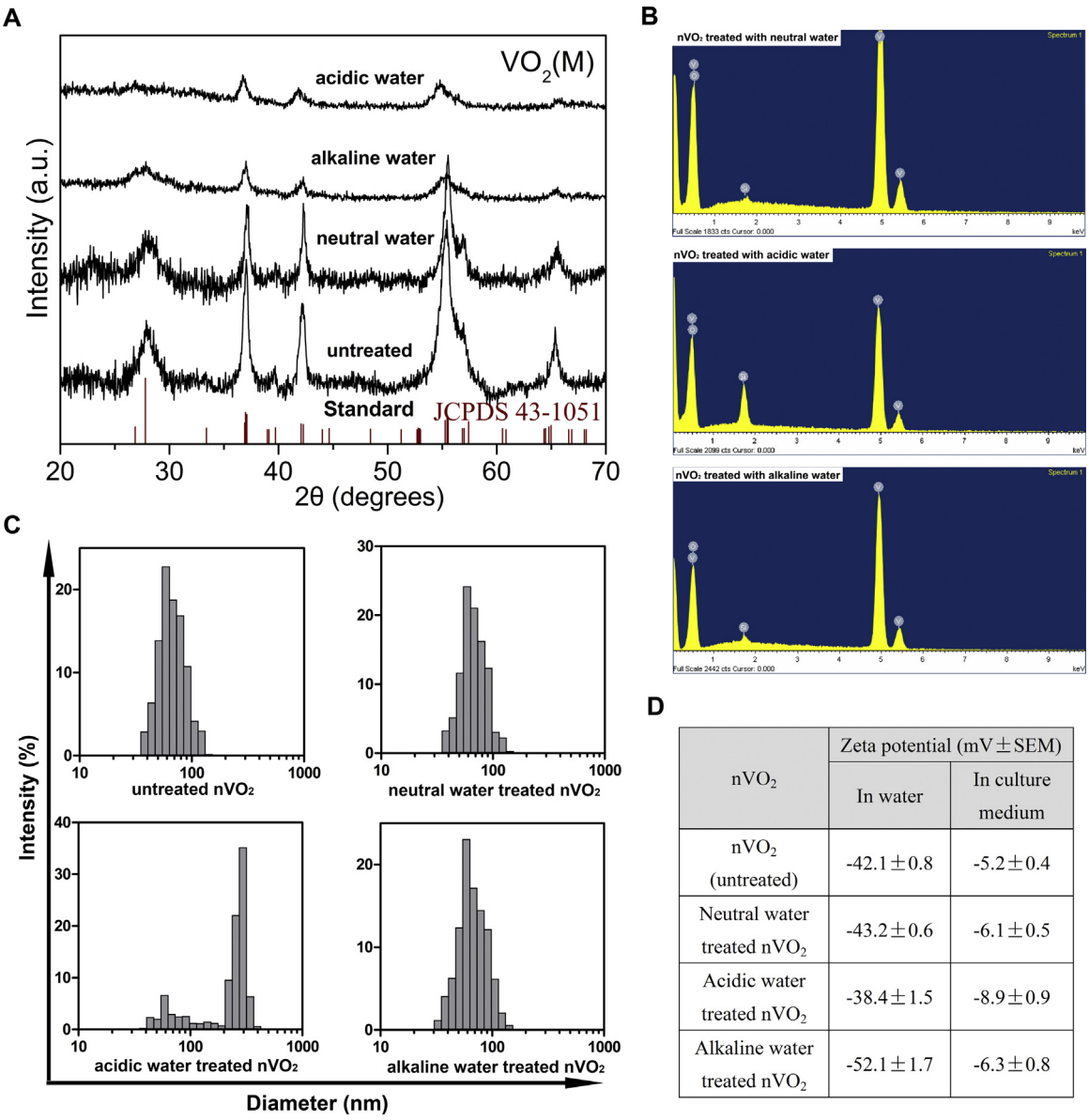

D

nVO_2	Zeta potential (mV±SEM)	
	In water	In culture medium
nVO_2 (untreated)	-42.1±0.8	-5.2±0.4
Neutral water treated nVO_2	-43.2±0.6	-6.1±0.5
Acidic water treated nVO_2	-38.4±1.5	-8.9±0.9
Alkaline water treated nVO_2	-52.1±1.7	-6.3±0.8

Fig. 3. The crystal structure and composition of nVO_2's transformation products (exposure for two weeks) by XRD and EDX. (A) The crystal structure was characterized by XRD. (B) The elementary composition was characterized EDX. (B) The hydrodynamic size and charge were displayed in (C and D), respectively.

5.2. The acidic transformed nVO_2 rapidly induced macrophage cell death mainly by apoptosis

To explore the biological effect of the acidic transformed nVO_2, we first measured its toxicity to different types of cell lines. Although neither pristine nor transformed nVO_2 was obviously toxic to HEK293T cells after treated with different doses for 24–48 h (Fig. S2A and Fig S3A), the transformed nVO_2 displayed an acute toxicity to macrophage RAW264.7 cells and BMDMs (Fig. 4, Fig. S2B, and Fig. S3B). The differences among cell lines might due to cell sensitivity, phagocytosis, and other immune characteristics of macrophage [21]. In trypan blue exclusion assay, after exposure to nVO_2 for 24 h, there was a sharp decrease in live cell number only after exposure to acidic transformed nVO_2 (5 μg/ml or 10 μg/ml). MTT assay was also explored to study the toxic change of nVO_2 after transformation. Data in Fig. 4B demonstrated that the toxicity of transformed nVO_2 increased with treatment time.

Next, we distinguished the cell death pattern using FITC-conjugated annexin V and PI staining as previously described [33]. As shown in Fig. 4C, at the time point of as earlier as 12 h, in the group that treated with transformed nVO_2, there was an obvious increase in the population labeled as annexin V^+ PI^-. Furthermore, PI staining on fixed cells, which represents a late phase detection index of the progress of apoptosis, also displayed that sub-G1 cell (apoptosis) populations increased in the group treated with transformed nVO_2 (Fig. 4D). These results demonstrated that the macrophage death induced by transformed nVO_2 was mainly apoptosis.

The acidic transformated nVO_2 induced Ca^{2+} enflux and loss of mitochondrial transmembrane potential ($\Delta\psi_m$) that parallels the progression of apoptosis

Apoptosis can be triggered by several pathways: the extrinsic pathway signaling through death receptors such as Fas/CD95 and TNFR [34], the intrinsic pathway characterized by mitochondrial membrane permeabilization (MMP), and pathway mediated by flux of Ca^{2+} from endoplasmic reticulum (ER) stores [35]. Several (immune) cell death receptor can initiate death signaling in macrophages [34], here, we checked the TNF-α/TNF-α receptor

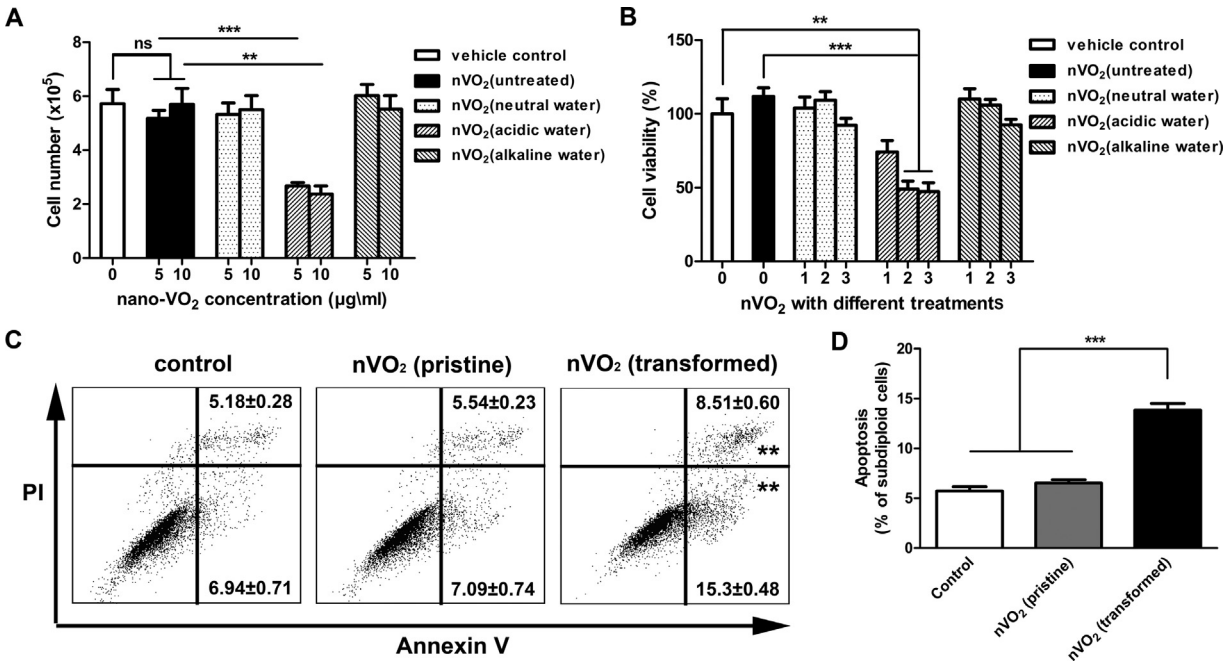

Fig. 4. The acidic transformed nVO_2 in acidic water induced macrophage cell death mainly by apoptosis. (A) Viability of macrophages treated with nVO_2 (pristine or transformed) at 5 to 10 μg/ml for 24 h was estimated by trypan blue exclusion assay; live cell number was counted. (B) Different pH-treated nVO_2 (for 1–3 weeks) were obtained and exposed to RAW 264.7 cells. Cell viability was assayed by using MTT. (C) Annexin V/PI staining was performed for displaying the apoptotic or dead cells after exposure to either pristine or transformed nVO_2 (10 μg/ml for 12 h). (D) After exposure, fixed cells were stained with PI and% of subdiploid cells was shown. Representative of at least 3 independent experiments ($n \geq 3$).

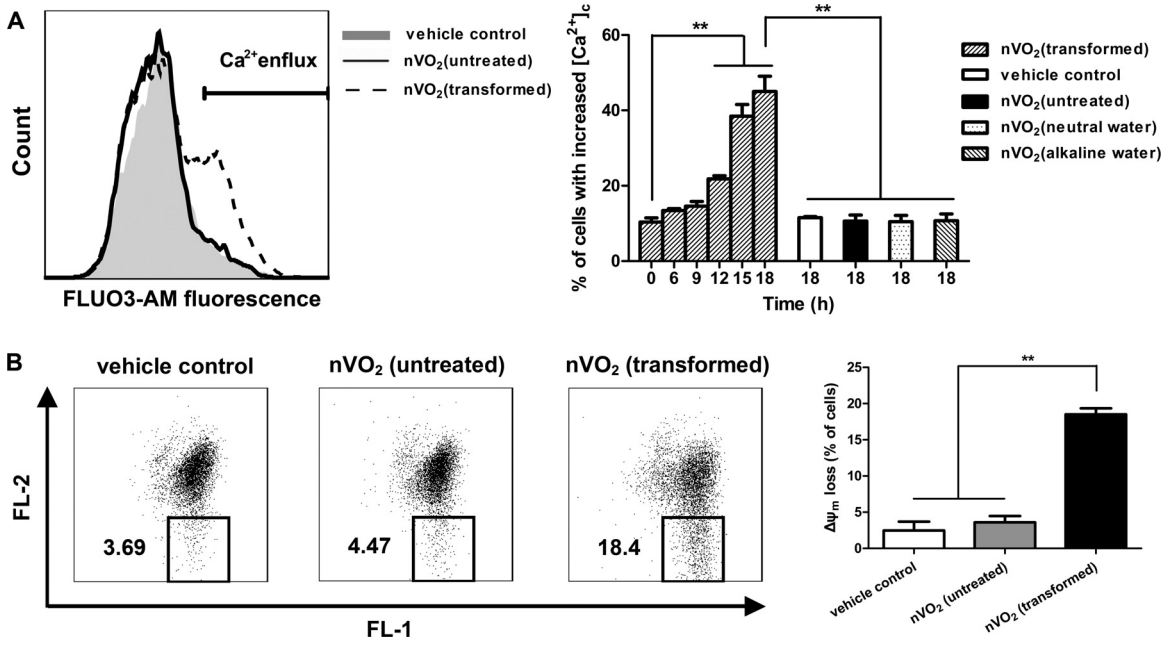

Fig. 5. Acidic transformed nVO_2 induced an increase in cytosolic Ca^{2+} concentration and a loss of mitochondrial transmembrane potential ($\Delta\psi m$) that parallels the progression of apoptosis. (A) RAW 264.7 cells were exposed to either pristine or transformed nVO_2 (at 10 μg/ml) from 0 to 18 h, stained with FLUO3-AM, and the fluorescence was quantified by flow cytometry. A 12 h-experiment was presented on left, and cells with increased cytosolic Ca^{2+} were gated. The time-dependent statistical result was shown on the right side. (B) Macrophages that exposure to 10 μg/ml of either pristine or transformed nVO_2 for 12 h were stained with JC-1 reagent, and assayed by flow cytometry. Cells attenuated in red fluorescence were gated, and the statistical result was shown on the right. Representative of at least 3 independent experiments ($n \geq 3$).

pathway, a common cell death route in macrophage, in the initial stage of macrophage apoptosis. Fig. S4 showed that the cell death caused by new transformation product was not attenuated upon pretreatment with the antagonist of TNF-α/TNF-α receptor (the WP9QY peptide) after exposure to nVO_2 for 12 h, suggesting that the TNF-α/TNFR did not participate in the transformation product induced apoptosis.

Next, we investigated whether the new transformation product modulated the cytosolic Ca^{2+} in macrophages using the calcium-sensitive dye FLUO3-AM. As shown in Fig. 5A, after 12 h exposure to different pH-treated nVO_2, a significant increase of cytosolic Ca^{2+} concentration was observed in cells exposure to transformed nVO_2 (in acidic water). A detailed experiment from 6 to 18 h displayed a time-dependent increase in the percentage of cells with

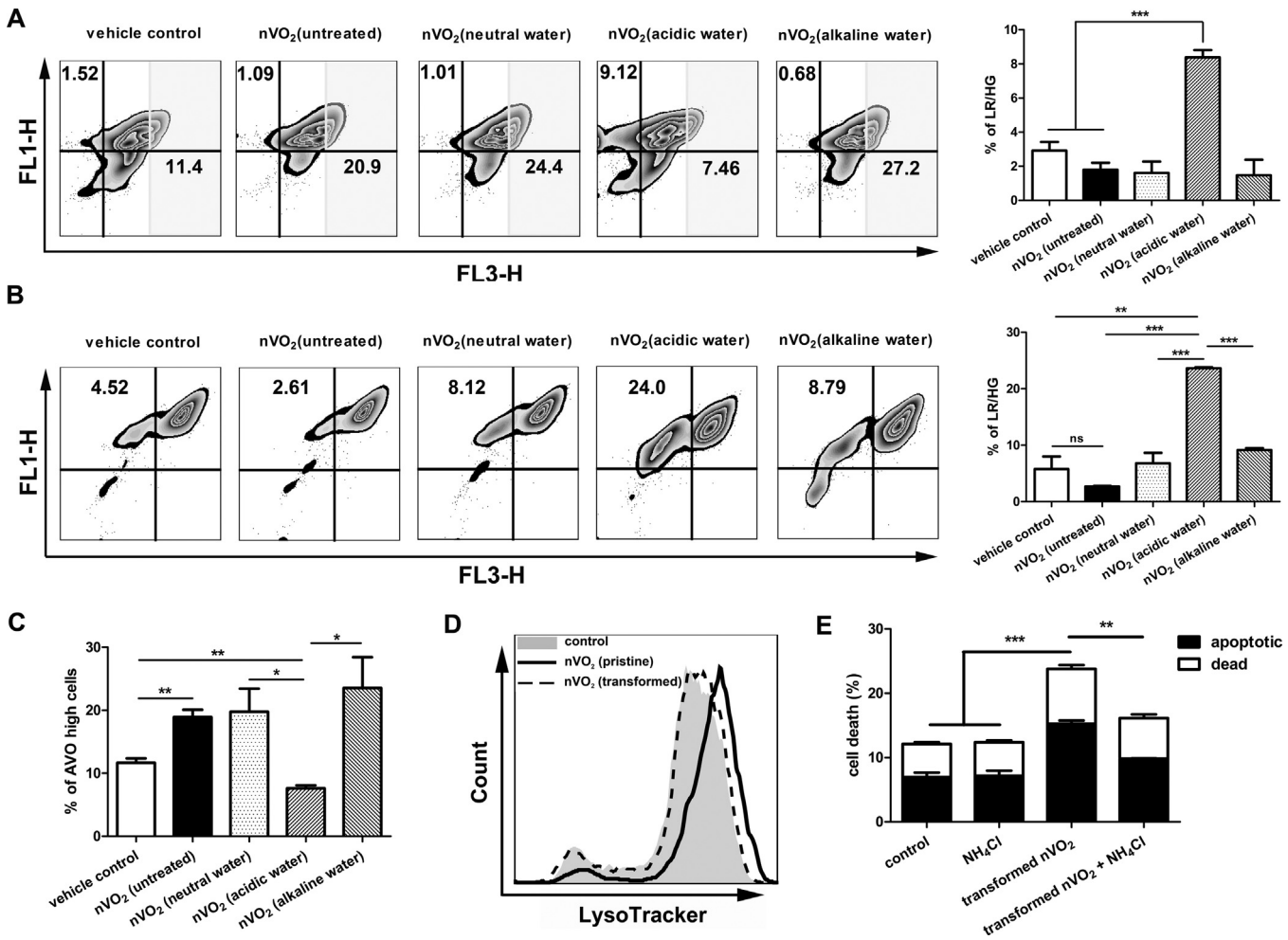

Fig. 6. Acidic transformed nVO_2 induced LMP in macrophage. (A) RAW 264.7 cells were prestained with AO, and then exposed to 10 μg/ml nVO_2 (pristine or transformed) for 6 h. AO fluorescence was analyzed by flow cytometry, and the subpopulation with low red and high green (LR/HG) fluorescence was gated with a quad gate. Percentage of this subpopulation was showed. (B) The same experiment (as in A) at 12 h displayed that the percentage of this subpopulation increased with time. Statistical results were shown on the right side (A, B). (C) The high red fluorescence subpopulation in A and B was gated (the shadow region) to show the AVOs. (D) RAW 264.7 cells were incubated with complete medium containing 50 nM Lysotracker Green at 37 °C for 60 min, washed and treated with nVO_2 for 12 h; cells were assayed using flow cytometry. (E) We pretreated RAW 264.7 cells with NH_4Cl (10 mM) for 1 h prior to 10 μg/ml nVO_2. Cells were then stained with Annexin V/PI, and assayed by flow cytometry to show apoptotic and dead cells. Representative of at least 3 independent experiments ($n \geq 3$).

high cytosolic Ca^{2+} concentration. These results indicated that the cytosolic Ca^{2+} concentration increased in parallel with apoptosis.

To further find out whether efflux of cytosolic Ca^{2+} to mitochondria induced the loss of mitochondrial transmembrane potential ($\Delta\psi_m$) and later MMP with the release of proapoptotic molecules [35], $\Delta\psi_m$ was measured using the JC-1 reagent. As shown in Fig. 5B, upon treatment with acidic transformed nVO_2, the gated cell population displayed a decrease in red fluorescence, implying an impairment of mitochondria and $\Delta\psi_m$ drop. All together, these results demonstrated that the transformed nVO_2 induced cell death at least by flux of Ca^{2+} from ER stores and MMP.

5.3. *The acidic transformated nVO_2 caused macrophage cell death by the induction of lysosomal membrane permeabilization (LMP)*

Lysosome can be affected before cells undergo apoptosis, especially for macrophages exposure to nanomaterials [36]. Studies showed that toxicants, such as anthrax lethal toxin, could induce LMP and cytosolic cathepsin release in macrophage [31], and lysosome-initiated apoptosis was followed by MMP [30]. To find whether lysosomes were impaired upon exposure to the transformation product of nVO_2, lysosomal acidity was analyzed using acridine orange (AO) staining [31]. As shown in Fig. 6A, LMP occurred in macrophage upon exposure to this transformation product as early as within 6 h (Fig. 6A, the subpopulation with low red and high green (LR/HG) fluorescence represented cells that underwent LMP), indicating that LMP was the initiating step during the progression of cell death. A longer time-point study at 12 h showed that LMP intensified in macrophages exposure to transformed nVO_2 (Fig. 6B). Additionally, experimental groups treated with pristine nVO_2 displayed a significant increase in the percentage of AVO high cells (Fig S5, Fig. 6C). This finding is consistent with previous study, both indicating that pristine nVO_2 induces autophagy [17].

In order to determine that the decrease in acidic compartments measured by AO was not caused by other processes [26,32,33], we employed the lysotracker dye, which labels acidic spherical granules within cells (but not lysosome-specific). Basically, when added prior to stimuli, lysotracker will continue to stain lysosomal membranes that undergo LMP; thus the fluorescence will change when lysosomal loss or fusion occurs during exocytosis, autophagy, or disintegration of lysosomal membranes [37]. Data in Fig. 6D showed that transformed nVO_2 did not induce a decrease in the lysotracker fluorescence intensity after 12 h treatment. This result

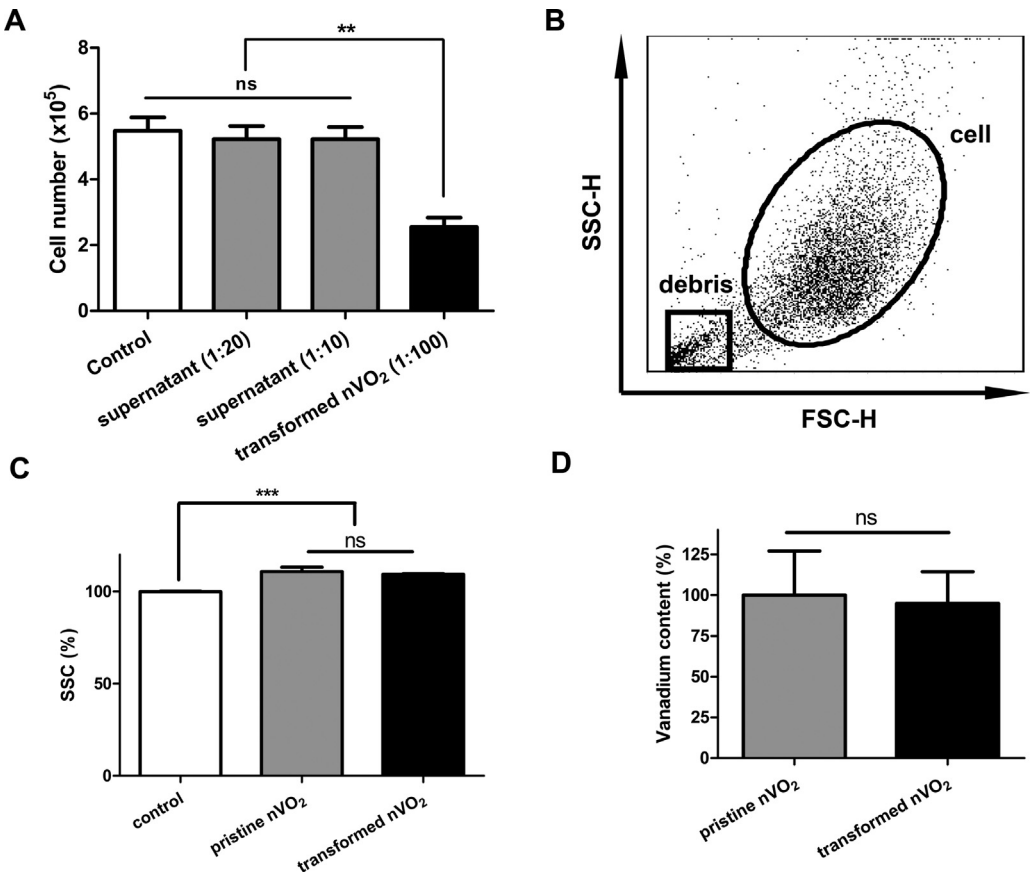

Fig. 7. Cellular uptake of pristine or transformed nVO_2 by RAW264.7 displayed no difference. (A) Supernatant or transformed nVO_2 itself was exposed to RAW264.7 cells for 24 h, (the supernatant of 1 mg/ml washed transformed nVO_2 was diluted to 1:10 or 1:20 for treatment, and 1 mg/ml transformed nVO_2 was added 1:100 to culture for obtain of a final concentration of 10 μg/ml). Live cell was estimated by trypan blue exclusion assay. (B) RAW264.7 cells were treated with 10 μg/ml of pristine or transformed nVO_2 for 12 h. Cells were assayed by flow cytometry. The elliptical gate displayed the main cell group while the rectangular displayed cell debris containing nVO_2. (C) SSC of cells treated with pristine or transformed nVO_2 for 12 h was displayed. (D) After treated with 10 μg/ml of pristine or transformed nVO_2 for 12 h, cells were sorted by flow cytometry, and their vanadium content was determined by ICP-MS.

indicated that decrease in acidic compartments measured by AO was not influenced by lysosomal loss or fusion.

Following permeabilization (LMP), lysosomal proteins such as effector protease cathepsins, leak into the cytosol and induce cell death [30]. Alkalinization of lysosomes with NH_4Cl can reduce the activity of lysosomal enzymes such as cathepsins [38]. Therefore, we wondered whether NH_4Cl pretreatment attenuated cell death in our experiment. As expected, pretreatment of cells with NH_4Cl (10 mM) for 1 h dramatically decreased cell death induced by transformed nVO_2 (Fig. 6E). This result demonstrated that the transformed nVO_2-induced macrophage cell death was mainly caused by LMP and the leakage of lysosomal effector proteases.

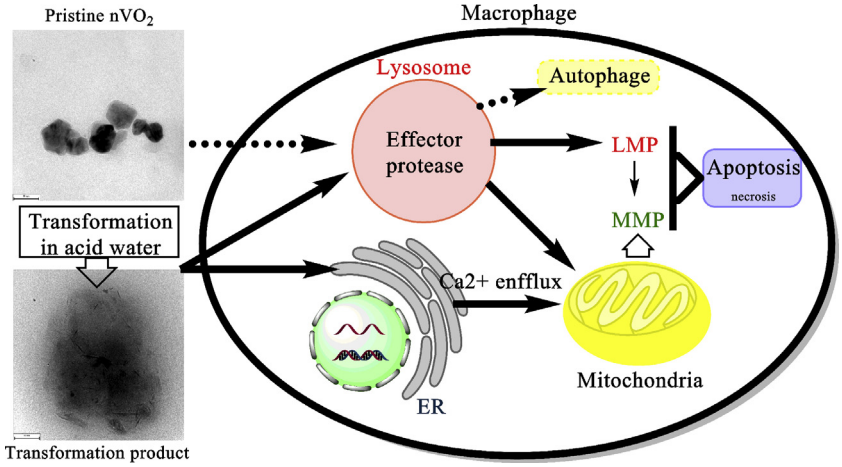

Fig. 8. Schematic of the toxicity mechanism of nVO_2's acidic transformation product to macrophage was displayed. The acidic transformed nVO_2 induces macrophage apoptosis by the induction of LMP and Ca^{2+} efflux.

5.4. Dissociated ions and cellular uptake level were not responsible for the acidic transformated nVO_2-induced cell death

To find whether the differences in toxicity induced by pristine or transformed VO_2 were caused by the dissociated ions, we exposed the supernatant (which contain dissociated ions) or transformed nVO_2 itself to RAW264.7 cells for 24 h, respectively (Fig. 7A). No obvious toxicity was observed in the supernatant-treated groups. Thus, the acidic transformated nVO_2-induced cell death was not due to any residual dissociated ions, as even a large amount of the supernatant of the transformed nVO_2 was non-toxic to RAW264.7 cells. Next, we investigated the cellular uptake level of pristine or transformed VO_2 by RAW264.7 cells using flow cytometry (Fig. 7B). The side scatter (SSC) of cells treated with pristine or transformed nVO_2 for 12 h changed significantly in relative to control cells; however, groups between pristine and transformed nVO_2 displayed no difference (Fig. 7C). The cellular uptake level of pristine and transformed nVO_2 had no significant change as determined by ICP-MS (Fig. 7D). Therefore, cellular uptake level of nVO_2 was not responsible for the acidic transformated nVO_2-induced cell death.

6. Discussion

Though the distinctive physicochemical properties of nanomaterials enable them to play an important role in all aspects of human life and social production, they also lead to adverse effects correlating with the small size-effect and surface-effect [39,40]. Nanomaterials change easily upon releasing into environment, especially in water systems. For instance, fullerene underwent surface oxidation and transformed to more soluble product in water; after entering into water systems, nano-Ag could be easily oxidized, resulting in increased toxicity to living system. These environmental transformations strongly affected biological effects of nanomaterials. For example, the toxicity of nano-ZnO to *Eisenia fetida* was highly influenced by pH [20]. Nano amphoteric oxides could easily transform under environmental factors, and the transformation products displayed distinctive biological effects [10].

nVO_2 has been widely applied in electrical/optical devices because of its outstanding thermochromic characteristics and MIT property [13,37]. Research demonstrated that nVO_2 induced autophagy in Hela cells [17]; however, there is little study concerning the toxicity of nVO_2 affected by environmental factors. Here, we demonstrate that nVO_2 aggregates together to form a new transformation product under acidic water condition for two weeks. And acidic transformed nVO_2 causes an acute toxicity to macrophages but not to epithelial cells. The specialized toxicity of transformed nVO_2 to macrophage suggests that immunotoxicity of nanoparticles is strongly influenced by environmental factors [41].

Several studies displayed that nanomaterials activated different signaling pathways to initiate cell death [27]. For instance, graphene oxide targeted TLR4 and resulted in TNF-R-induced programmed necrosis in macrophages, and nano-ZnO quickly initiated ER stress response before inducing apoptosis [21,42]. In order to clarify the underlying mechanism of macrophage cell death mediated by transformed nVO_2, we checked several pathways triggering cell death. We found that transformed nVO_2 induced an increase in cytosolic Ca^{2+} concentration and loss of $\Delta\psi_m$ that parallels the progression of apoptosis. These results indicated that ER was suffered at the initiate stage during transformed nVO_2-induced cell death. The finding is consistent with the report displaying that nano-ZnO could interrupt ER homeostasis before inducing apoptosis [27].

Nanomaterials enter cytoplasm and different organelles where they cause damage [27,42,43]. In the present study, we showed that besides ER and mitochondria, lysosome was suffered upon exposure to transformed nVO_2 [31,44]. LMP is an initiating step during the progression of cell death under several conditions. For example, lysosomal rupture is an early event in p53-induced apoptosis [45]. Lysosome also suffered by cytotoxic stimulus: silica, or even ROS, can modulate lysosomal enzyme activity and induce apoptosis in macrophages [38,46]. In this work, by employing AO and lysotracker staining, we confirmed that lysosomal function was impaired and LMP occurred at the early stage upon exposure to transformed nVO_2. This process was earlier than Ca^{2+} efflux and MMP, indicating that the lysosome-initiated apoptosis later initiated MMP [30]. Besides, alkalinization of lysosomes by pretreating cells with NH_4Cl, which can reduce the activity of lysosomal enzymes such as cathepsins, attenuated the cell death caused by transformed nVO_2. Therefore, we indicated that LMP was an initiating signal that induced Ca^{2+} efflux and loss of $\Delta\psi_m$ in our study, and leakage of lysosomal proteins into the cytosol might also promote cell death (Fig. 8).

In conclusion, we confirm that nVO_2 transforms during exposure to acidic water condition and its transformation product rapidly induces macrophage apoptosis by the induction of LMP and Ca^{2+} efflux. These findings indicate that pH affects nVO_2's physicochemical properties, thereby altering their toxicity. This work suggests that more attention should be paid to the influence of environmental factors when assessing the risk of metal oxide nanoparticles.

Acknowledgments

This work was supported by the National Basic Research Program of China (Grant no. 2014CB932002), the CAS Strategic Priority Research Program (XDB14030502), the CAS/SAFEA International Partnership Program for Creative Research Teams, and National Natural Science Foundation of China (20977093, 31470829 and81273004).

Appendix A. Supplementary data

Supplementary data associated with this article can be found, in the online version, at http://dx.doi.org/10.1016/j.toxrep.2015.06.005

References

[1] A.D. Maynard, R.J. Aitken, T. Butz, V. Colvin, K. Donaldson, G. Oberdorster, M.A. Philbert, J. Ryan, A. Seaton, V. Stone, S.S. Tinkle, L. Tran, N.J. Walker, D.B. Warheit, Safe handling of nanotechnology, Nature 444 (2006) 267–269.
[2] A. Nel, T. Xia, L. Madler, N. Li, Toxic potential of materials at the nanolevel, Science 311 (2006) 622–627.
[3] R. Werlin, J.H. Priester, R.E. Mielke, S. Kramer, S. Jackson, P.K. Stoimenov, G.D. Stucky, G.N. Cherr, E. Orias, P.A. Holden, Biomagnification of cadmium selenide quantum dots in a simple experimental microbial food chain, Nat. Nanotechnol. 6 (2011) 65–71.
[4] P. Ghafari, C.H. St-Denis, M.E. Power, X. Jin, V. Tsou, H.S. Mandal, N.C. Bols, X.S. Tang, Impact of carbon nanotubes on the ingestion and digestion of bacteria by ciliated protozoa, Nat. Nanotechnol. 3 (2008) 347–351.
[5] M.A. Kiser, D.A. Ladner, K.D. Hristovski, P.K. Westerhoff, Nanomaterial transformation and association with fresh and freeze–dried wastewater activated sludge: implications for testing protocol and environmental fate, Environ. Sci. Technol. 46 (2012) 7046–7053.
[6] J.L. Ferry, P. Craig, C. Hexel, P. Sisco, R. Frey, P.L. Pennington, M.H. Fulton, I.G. Scott, A.W. Decho, S. Kashiwada, C.J. Murphy, T.J. Shaw, Transfer of gold nanoparticles from the water column to the estuarine food web, Nat. Nanotechnol. 1 (-) (2009).
[7] T. Walser, L.K. Limbach, R. Brogioli, E. Erismann, L. Flamigni, B. Hattendorf, M. Juchli, F. Krumeich, C. Ludwig, K. Prikopsky, M. Rossier, D. Saner, A. Sigg, S. Hellweg, D. Gunther, W.J. Stark, Persistence of engineered nanoparticles in a municipal solid-waste incineration plant, Nat. Nanotechnol. 7 (2012) 520–524.
[8] C.T. Hou, Jafvert, Photochemical transformation of aqueous C60 clusters in sunlight, Environ. Sci. Technol. 43 (2009) 362–367.
[9] C. Wang, C. Shang, M. Ni, J. Dai, F. Jiang, (Photo) chlorination-induced physicochemical transformation of aqueous fullerene nC60, Environ. Sci. Technol. 46 (2012) 9398–9405.

[10] Y.C. M.M. Wang, X.N. Wang, Y. Wang, H. Liu, J.W. Zhang, Q. Zhang, S.P. Huang, T.K. Chen, L.J. Wu Hei, Mutagenicity of ZnO nanoparticles in mammalian cells: role of physicochemical transformations under the aging process, Nanotoxicology (2015), http://dx.doi.org/10.3109/17435390.2014.992816
[11] M. Li, X. Wu, L. Li, Y.X. Wang, D.B. Li, J. Pan, S.J. Li, L.T. Sun, G.H. Li, Defect-mediated phase transition temperature of VO_2 (M) nanoparticles with excellent thermochromic performance and low threshold voltage, J. Mater. Chem. A 2 (2014) 4520–4523, 2.
[12] F.L. Assem, L.S. Levy, A review of current toxicological concerns on vanadium pentoxide and other vanadium compounds: gaps in knowledge and directions for future research, J. Toxicol. Environ. Health B Crit. Rev. 12 (2009) 289–306.
[13] T.I. Fortoul, M. Rojas-Lemus, V. Rodriguez-Lara, A. Gonzalez-Villalva, M. Ustarroz-Cano, G. Cano-Gutierrez, S.E. Gonzalez-Rendon, L.F. Montano, M. Altamirano-Lozano, Overview of environmental and occupational vanadium exposure and associated health outcomes: an article based on a presentation at the 8th International Symposium on Vanadium Chemistry, Biological Chemistry, and Toxicology, Washington DC, August 15–18, J. Immunotoxicol. 11 (2014) 13–18.
[14] Y. Shechter, S.J. Karlish, Insulin-like stimulation of glucose oxidation in rat adipocytes by vanadyl (IV) ions, Nature (1980) 556–558, 2.
[15] L.C.M.D. Cantley Resh Jr., G. Guidotti, Vanadate inhibits the red cell (Na^+, K^+) ATPase from the cytoplasmic side, Nature 272 (1978) 552–554.
[16] G.L. Schieven, A.F. Wahl, S. Myrdal, L. Grosmaire, J.A. Ledbetter, Lineage-specific induction of B-cell apoptosis and altered signal-transduction by the phosphotyrosine phosphatase inhibitor bis(maltolato) oxovanadium(Iv), J. Biol. Chem. 270 (1995) 20824–20831.
[17] W. Zhou, Y.Y. Miao, Y.J. Zhang, L. Liu, J. Lin, J.Y. Yang, Y. Xie, L.P. Wen, Induction of cyto-protective autophagy by paramontroseite VO_2 nanocrystals, Nanotechnology 24 (2013).
[18] J.M. Worle-Knirsch, K. Kern, C. Schleh, C. Adelhelm, C. Feldmann, H.F. Krug, Nanoparticulate vanadium oxide potentiated vanadium toxicity in human lung cells, Environ. Sci. Technol. 41 (2007) 331–336.
[19] S.W. Bian, I.A. Mudunkotuwa, T. Rupasinghe, V.H. Grassian, Aggregation and dissolution of 4nm ZnO nanoparticles in aqueous environments: influence of pH, ionic strength, size, and adsorption of humic acid, Langmuir 27 (2011) 6059–6068.
[20] L.R. Heggelund, M. Diez-Ortiz, S. Lofts, E. Lahive, K. Jurkschat, J. Wojnarowicz, N. Cedergreen, D. Spurgeon, C. Svendsen, Soil pH effects on the comparative toxicity of dissolved zinc, non-nano and nano ZnO to the earthworm *Eisenia fetida*, Nanotoxicology 8 (2013) 559–572.
[21] G. Qu, S. Liu, S. Zhang, L. Wang, X. Wang, B. Sun, N. Yin, X. Gao, T. Xia, J.J. Chen, G.B. Jiang, Graphene oxide induces toll-like receptor 4 (TLR4)-dependent necrosis in macrophages, ACS Nano 7 (2013) 5732–5745.
[22] X.D. Li, Y.H. Chiu, A.S. Ismail, C.L. Behrendt, M. Wight-Carter, L.V. Hooper, Z.J. Chen, Mitochondrial antiviral signaling protein (MAVS) monitors commensal bacteria and induces an immune response that prevents experimental colitis, Proc. Natl. Acad. Sci. U. S. A. 108 (2011) 17390–17395.
[23] A.M. El Badawy, T.P. Luxton, R.G. Silva, K.G. Scheckel, M.T. Suidan, T.M. Tolaymat, Impact of environmental conditions (pH, ionic strength, and electrolyte type) on the surface charge and aggregation of silver nanoparticles suspensions, Environ. Sci. Technol. 44 (2010) 1260–1266.
[24] A. Paul, R. Stosser, A. Zehl, E. Zwirnmann, R.D. Vogt, C.E. Steinberg, Nature and abundance of organic radicals in natural organic matter: effect of pH and irradiation, Environ. Sci. Technol. 40 (2006) 5897–5903.
[25] M. Li, S.L. Ji, J. Pan, H. Wu, L. Zhong, Q. Wang, F.D. Li, G.H. Li, Infrared response of self-heating VO_2 nanoparticles film based on Ag nanowires heater, J. Mater. Chem. A. 2 (2014) 20470–20473.
[26] X. Yang, C. Jiang, H. Hsu-Kim, A.R. Badireddy, M. Dykstra, M. Wiesner, D.E. Hinton, J.N. Meyer, Silver nanoparticle behavior, uptake, and toxicity in *Caenorhabditis elegans*: effects of natural organic matter, Environ. Sci. Technol. 48 (2014) 3486–3495.
[27] W.S. Cho, R. Duffin, M. Bradley, I.L. Megson, W. MacNee, J.K. Lee, J. Jeong, K. Donaldson, Predictive value of in vitro assays depends on the mechanism of toxicity of metal oxide nanoparticles, Part Fibre Toxicol. 10 (2013) 55.
[28] I. Riccardi, Nicoletti, Analysis of apoptosis by propidium iodide staining and flow cytometry, Nat. Protoc. 1 (2006) 1458–1461.
[29] C. Brisac, F. Teoule, A. Autret, I. Pelletier, F. Colbere-Garapin, C. Brenner, C. Lemaire, B. Blondel, Calcium flux between the endoplasmic reticulum and mitochondrion contributes to poliovirus-induced apoptosis, J. Virol. 84 (2010) 12226–12235.
[30] P. Boya, G. Kroemer, Lysosomal membrane permeabilization in cell death, Oncogene 27 (2008) 6434–6451.
[31] K.M. Averette, M.R. Pratt, Y.A. Yang, S. Bassilian, J.P. Whitelegge, J.A. Loo, T.W. Muir, K.A. Bradley, Anthrax lethal toxin induced lysosomal membrane permeabilization and cytosolic cathepsin release is Nlrp1b/Nalp1b-dependent, PLoS One 4 (2009).
[32] Y.J. Ma, S. Elankumaran, L.C. Marr, E.P. Vejerano, A. Pruden, Toxicity of engineered nanomaterials and their transformation products following wastewater treatment on A549 human lung epithelial cells, Toxicol. Rep. 1 (2014) 871–876.
[33] P.V. AshaRani, G. Low Kah Mun, M.P. Hande, S. Valiyaveettil, Cytotoxicity and genotoxicity of silver nanoparticles in human cells, ACS Nano 3 (2009) 279–290.
[34] H. Wajant, The Fas signaling pathway: more than a paradigm, Science 296 (2002) 1635–1636.
[35] P. Pinton, C. Giorgi, R. Siviero, E. Zecchini, R. Rizzuto, Calcium and apoptosis: ER-mitochondria Ca^{2+} transfer in the control of apoptosis, Oncogene 27 (2008) 6407–6418.
[36] S.T. Stern, P.P. Adiseshaiah, R.M. Crist, Autophagy and lysosomal dysfunction as emerging mechanisms of nanomaterial toxicity, Part Fibre Toxicol. 9 (2012) 20.
[37] S.W. Tait, D.R. Green, Mitochondria and cell death: outer membrane permeabilization and beyond, Nat. Rev. Mol. Cell Biol. 11 (2010) 621–632.
[38] M.S. Thibodeau, C. Giardina, D.A. Knecht, J. Helble, A.K. Hubbard, Silica-induced apoptosis in mouse alveolar macrophages is initiated by lysosomal enzyme activity, Toxicol. Sci. 80 (2004) 34–48.
[39] U.S. Akhtar, N. Rastogi, R.D. McWhinney, B. Urch, C.W. Chow, G.J. Evans, J.A. Scott, The combined effects of physicochemical properties of size-fractionated ambient particulate matter on in vitro toxicity in human A549 lung epithelial cells, Toxicol. Rep. 1 (2014) 145–156.
[40] H.M. Braakhuis, M.V. Park, I. Gosens, W.H. De Jong, F.R. Cassee, Physicochemical characteristics of nanomaterials that affect pulmonary inflammation, Part Fibre Toxicol. 11 (2014) 18.
[41] M.A. Dobrovolskaia, S.E. McNeil, Immunological properties of engineered nanomaterials, Nat. Nanotechnol. 2 (2007) 469–478.
[42] R. Chen, L. Huo, X. Shi, R. Bai, Z. Zhang, Y. Zhao, Y. Chang, C. Chen, Endoplasmic reticulum stress induced by zinc oxide nanoparticles is an earlier biomarker for nanotoxicological evaluation, ACS Nano 8 (2014) 2562–2574.
[43] Y. Chen, Z. Wang, M. Xu, X. Wang, R. Liu, Q. Liu, Z. Zhang, T. Xia, J. Zhao, G. Jiang, Y. Xu, S. Liu, Nanosilver incurs an adaptive shunt of energy metabolism mode to glycolysis in tumor and nontumor cells, ACS Nano 8 (2014) 5813–5825.
[44] L. Verschooten, K. Barrette, S. Van Kelst, N.R. Romero, C. Proby, R. De Vos, P. Agostinis, M. Garmyn, Autophagy inhibitor chloroquine enhanced the cell death inducing effect of the flavonoid luteolin in metastatic squamous cell carcinoma cells, PLoS One 7 (2012).
[45] X.M. Yuan, W. Li, H. Dalen, J. Lotem, R. Kama, L. Sachs, U.T. Brunk, Lysosomal destabilization in p53-induced apoptosis, Proc. Natl. Acad. Sci. U. S. A. 99 (2002) 6286–6291.
[46] A. Terman, T. Kurz, B. Gustafsson, U.T. Brunk, Lysosomal labilization, IUBMB Life 58 (2006) 531–539.